J. Membrane Biol. 190, 93–103 (2002)
DOI: 10.1007/s00232-002-1027-3

The Journal of
Membrane
Biology

Structural Implications of Placing Cationic Residues at either the NH_2- or COOH-Terminus in a Pore-forming Synthetic Peptide

J.R. Broughman[1]*, L.P. Shank[1], O. Prakash[1], B.D. Schultz[2], T. Iwamoto[1], J.M. Tomich[1], K. Mitchell[2]
[1]Department of Biochemistry, 104 Willard Hall, Kansas State University, Manhattan, KS 66506, USA
[2]Department of Anatomy and Physiology, 228 Coles Hall, Kansas State University, Manhattan, KS 66506, USA

Received: 30 March 2002/Revised: 9 July 2002

Abstract. Restoration of chloride conductance via introduction of an anion-selective pore, formed by a channel-forming peptide, has been hypothesized as a novel treatment modality for patients with cystic fibrosis. Delivery of these peptides from an aqueous environment in the absence of organic solvents is paramount. M2GlyR peptides, designed based on the glycine receptor, insert into lipid bilayers and polarized epithelial cells and assemble spontaneously into chloride-conducting pores. Addition of 4 lysine residues to either terminus increases the solubility of M2GlyR peptides. Both orientations of the helix within the membrane form an anion-selective pore, however, differences in solubility, associations and channel-forming activity are observed. To determine how the positioning of the lysine residues affects these properties, structural characteristics of the lysyl-modified peptides were explored utilizing chemical cross-linking, NMR and molecular modeling. Initial model structures of the α-helical peptides predict that lysine residues at the COOH-terminus form a capping structure by folding back to form hydrogen bonds with backbone carbonyl groups and hydroxyl side chains of residues in the helical segment of the peptide. In contrast, lysine residues at the NH_2-terminus form fewer H-bonds and extend away from the helical backbone. Results from NMR and chemical cross-linking support the model structures. The C-cap formed by H-bonding of lysine residues is likely to account for the different biophysical properties observed between NH_2- and COOH-terminal-modified M2GlyR peptides.

Key words: Helix capping — Glycine receptor — Anion transport — Synthetic channel-forming peptide — Channel replacement therapy — Cystic fibrosis

Introduction

Peptide-based channel-replacement therapy is a potentially useful method for addressing human diseases such as cystic fibrosis (CF)[1] that are caused by a loss of channel function. This approach also permits evaluation of the role of anion secretion in the pathology of the CF disease process. A human-derived CF cell line (CFT1) incubated with NK_4-M2GlyR exhibited a restoration of both anion secretion and glutathione transport (Gao et al., 2001). This proposed treatment modality lies midway between conventional drug therapy and gene therapy. In the case of cystic fibrosis, currently approved conventional drug therapy addresses only symptoms such as inflammation, mucus accumulation and bacterial infection. Gene therapy, though not approved, addresses the root cause of the disorder but requires

**Current address:* Department of Anatomy and Physiology, 228 Coles Hall Kansas State University, Manhattan, KS 66506.

Correspondence to: K.E. Mitchell; email: mitchell@vet.ksu.edu

[1]Abbreviations: AchR, acetylcholine receptor; BS^3, Bis[sulfosuccinimidyl]suberate; CF, cystic fibrosis; CFP, channel-forming peptide; DMEM, Dulbecco's Modified Eagle Medium; DMSO, dimethyl sulfoxide; 1-EBIO, 1-ethyl-2-benzimidazolinone; FBS, fetal bovine serum; Fmoc, fluoren-9-yl methoxycarbonyl; HEPES, 4-(2-hydroxyethyl) piperazine-1-ethanesulfonic acid; HMP, *p*-hydroxymethylphenoxymethyl; HPLC, high performance liquid chromatography; I_{SC}, short circuit current; MALDI-TOF, matrix assisted-laser desorption time-of-flight mass spectroscopy; MDCK, Madin-Darby canine kidney cells; M2GlyR, second transmembrane segment of the glycine receptor; NOESY, nuclear Overhauser effect spectroscopy; PAGE, polyacrylamide gel electrophoresis; SDS, sodium dodecylsulfate; TFE, trifluoroethanol; TOCSY, total correlation spectroscopy.

stable transfection as well as all of the cell's transcriptional, translational and post translational processing to place a functional protein in the apical membrane of airway epithelium. Peptide-based channel replacement therapy for cystic fibrosis, also in the developmental stage, involves merely applying the peptide to the apical surface of the airway epithelium (the air/cell interfacial membrane). Once bound to the target membrane, the peptide inserts across the bilayers and assembles into functional ion conductive pores.

Developing new amphipathic peptides that retain channel-forming activity with improved aqueous solubility and decreased solution propensity to form high molecular weight associations is a key objective in making "peptide-based channel replacement therapy" a reality. Throughout the search for a lead CF therapeutic, an iterative process has been employed to identify peptide sequences that are highly soluble in aqueous solution, yet retain the ability to form functional channels in epithelial cell membranes. The studies presented in this report detail experiments that show the structural consequences of manipulating the position of the lysine adducts or the sequential removal of amino acids at either the COOH- or NH_2-terminus. It is clear from the present work that separate and discrete segments exist within the M2GlyR sequence, which direct solution peptide-peptide association and membrane assembly of these sequences. Removal of the association domain greatly enhances the population of monomer with enhanced channel-forming activity (Broughman et al., 2002).

A synthetic peptide based on the second transmembrane segment of the α1 subunit of the brain glycine receptor (M2GlyR; residues 284–306; PARVGLGITTVLTMTTQSSGSRA) is capable of assembly into chloride-selective pores (Reddy et al., 1993). The addition of four lysine residues to the COOH-(CK_4-M2GlyR) or the NH_2-terminus (NK_4-M2GlyR) results in increased aqueous solubility with retention of channel-forming activity (Tomich et al., 1998). CK_4-M2GlyR and NK_4-M2GlyR can form channels in planar lipid bilayers (Broughman et al., 2001; Mitchell et al., 2000), increase whole-cell chloride conductance in isolated epithelial cells (Broughman et al., 2001; Mitchell et al., 2000) and induce chloride secretion and water transport from epithelial cell monolayers (Broughman et al., 2001; Tomich et al., 1998; Wallace et al., 2000; Wallace et al., 1997).

Differences in both the biophysical and electrophysiological properties of the NH_2- *vs.* COOH-adducted peptides have been demonstrated previously. In separate experiments, the maximal increase in short-circuit current (I_{SC}, indicative of anion secretion) induced by treatment of epithelial monolayers with NK_4-M2GlyR is 50% greater than the increase in I_{SC} induced by CK_4-M2GlyR (Broughman et al., 2001; Wallace et al., 2000). In addition, NK_4-M2GlyR forms more stable channels in planar lipid bilayers than does CK_4-M2GlyR (Broughman et al., 2001; Mitchell et al., 2000). M2GlyR is hydrophobic and aggregates in aqueous solution; modification with lysine residues at either terminus results in increased aqueous solubility of both peptides. However, NK_4-M2GlyR is less soluble than CK_4-M2GlyR (13.4 mM *vs.* 27.5 mM, respectively) (Tomich et al., 1998). In Ringer solution, the shielding of the polar lysine residues of both peptides by ionic solutes results in the formation of soluble high molecular weight associations, as measured by increased viscosity of the peptides over time (Tomich et al., 1998). The time-dependent increase in viscosity for NK_4-M2GlyR follows a second-order process and produces peptide-peptide associations that are subject to shear. CK_4-M2GlyR, under identical conditions, displays viscosity increases that are first-order, forming associations less susceptible to shear. These differences in the biophysical properties of NK_4-M2GlyR and CK_4-M2GlyR likely result from differences in the structure of the peptides near the lysine tail and/or interactions of the lysine residues with the helical M2GlyR segment of the peptide.

NH_2- and COOH-terminal helix capping motifs are important in stabilizing secondary structure in proteins (Richardson & Richardson, 1988). The capping residues are thought to form H-bonds with the last four backbone carbonyl and amide groups at the helix termini. The uneven distribution of residues found at the ends of helices in proteins in nature suggests that some residues may be favored in helix-capping motifs (Richardson & Richardson, 1988). In particular, polar side chain-backbone interactions may be important (Aurora & Rose, 1998; Presta & Rose, 1988). COOH-terminal capping motifs have been proposed for synthetic peptides as well. A report (Zhou et al., 1994) described H-bonding interactions between the side-chain amide of an asparagine residue at the COOH-terminus of a synthetic α-helical peptide with the backbone carbonyl of a residue four positions further along the peptide chain. This resulted in a tightening of the COOH-terminus into a 3^{10} helix. In a similar study, a single lysine residue at the COOH-terminus of a synthetic 22-amino-acid channel-forming α-helical peptide was shown to distort the geometry of the helix at the COOH-terminus by interactions between the lysine amino group and the backbone carbonyl of a residue four positions further along the peptide chain (Esposito et al., 1997). Based on the significance of capping motifs in nature and the effects of polar side chains at the COOH-termini of synthetic peptides, we sought to explore how lysine residues at the COOH- *vs.* the NH_2-terminus of the M2GlyR sequence influence helical structure and thus activity.

CK_4-M2GlyR forms fewer cross-linked associations than NK_4-M2GlyR. This reduction in cross-

linking of CK_4-M2GlyR may be due to differences in orientation of the individual peptides within the associations, perturbations of the monomer structure that mask sequence elements that promote peptide-peptide associations or to lysine ε-amino groups that are less available to cross-linker reagents. NMR data suggest that the environments for the lysine residues are different for the two peptides. Molecular modeling and molecular dynamics were used to generate structures of the NK_4-M2GlyR and CK_4-M2GlyR peptides to explore these structures further. Initial model structures of the 27-amino-acid α-helical peptides predict that the four lysine residues, when at the COOH-terminus, form a capping structure by folding back to form H-bonds with backbone carbonyl groups and hydroxyl side chain groups of residues in the helical segment of the peptide. In contrast, the lysine residues at the NH_2-terminus extend away from the helix backbone and form fewer H-bonds with the helical segment of the peptide. The differences in the capping structures formed by lysine residues at the NH_2- and COOH-termini are likely to account for the different biophysical properties of the lysine-modified M2GlyR peptides including channel assembly, associations and solubility.

Materials and Methods

Peptide Synthesis

All peptides were synthesized by solid-phase synthesis using 9-fluorenyl methoxycarbonyl (Fmoc) chemistry on an ABI 431A peptide synthesizer (Perkin-Elmer, Norwalk, CT). *p*-Hydroxymethylphenoxymethyl (HMP) resin preloaded with the COOH-terminal amino acid was purchased from Perkin-Elmer, N-α-Fmoc-protected amino acids were purchased from Perkin-Elmer, Bachem (Torrence, CA), Peninsula Laboratories (Belmont, CA) and Peptides International (Louisville, KY). All peptides were characterized by reversed-phase HPLC and matrix assisted-laser desorption time-of-flight mass spectroscopy (MALDI-TOF).

Sequence	Name
KKKKPARVGLGITTVLTMTTQSSGSRA	NK_4-M2GlyR
PARVGLGITTVLTMTTQSSGSRAKKKK	CK_4-M2GlyR

Short-circuit Current Measurements

Madin-Darby canine kidney (MDCK) cells were maintained in culture as described previously in detail (Broughman et al., 2001; Wallace et al., 1997). For Ussing-chamber experiments, cells were seeded onto 1.13-cm^2 permeable supports (Snapwell, Costar, Cambridge, MA) at a density of approximately 1×10^6 cells/well and incubated in Dulbecco's Modified Eagle Medium with Ham's F12 nutrient mixture (DMEM/F-12), supplemented with fetal bovine serum (FBS) and antibiotics (changed every other day) for 2–3 weeks prior to being mounted in modified Ussing chambers. Transepithelial ion transport was evaluated in a modified Ussing chamber (Model DCV9, Navicyte, San Diego, CA) as described previously in detail (Broughman et al., 2001). I_{SC} data are from steady-state flux levels. Results are presented as mean ± SEM.

Chemical Cross-linking

Bis[Sulfosuccinimidyl]suberate (BS^3) (Pierce, Rockford, IL), a water-soluble homo-bifunctional cross-linking reagent that reacts with free amino groups, was made as a 200 mM stock solution in dimethyl sulfoxide (DMSO). Peptide stock solutions (1 mM) were made in distilled water. The cross-linking reactions were carried out by diluting the peptide stock solutions in 10 mM 4-(2-Hydroxyethyl)piperazine-1-ethanesulfonic acid (HEPES) buffer, pH 6.5, to a final concentration of 150 μM in a final volume of 97 μl. After equilibration of the diluted peptide solution at room temperature for 15 min, BS^3 (3 μl) was added to obtain a final concentration of 6 mM, resulting in a forty-fold molar excess of cross-linker over peptide. After 30 min, the cross-linking reaction was terminated by the addition of 1 N HCl (1:10). The reaction mix was dried under vacuum and dissolved in distilled water. The reaction mix was diluted in tricine-SDS sample buffer (50:50, v/v), and boiled for 5 min. The samples were resolved by electrophoresis on 10–20% tricine gels (Schagger & von Jagow, 1987) and visualized with silver staining (SilverXpress®, Invitrogen, Carlsbad, CA). Apparent molecular mass of the peptides was calculated from a standard curve made by plotting the $\log_{10}$ of the molecular mass of the known standard proteins versus the distance of migration.

NMR Spectroscopy

NMR Spectroscopy was performed as described previously (Vogen et al., 1998). High-resolution one- and two-dimensional ^{1}H-NMR experimental data were acquired on an 11.75 T Varian UNITYplus spectrometer (Varian, Palo Alto, CA) operating at 499.96 MHz for ^{1}H, with a 5-mm triple-resonance inverse detection probe. Spectra of peptides (3.0 mM) were recorded at 30°C in water containing 30% deuterated trifluoroethanol (TFE). Quantitative analysis of the CD measurements made in 30% TFE suggested 55% helical structure (Bohm, Muhr & Jaenicke, 1992). Further increases in TFE content did not change the percent helicity as measured by CD. Varian NMR software VNMR 6.1B on a Sun Microsystems Ultra 10 workstation was used for NMR data acquisition and analysis. A total of 256 increments of 4K data points were collected for these experiments. All data sets were obtained in hypercomplex phase-sensitive mode. Proton resonance assignments were confirmed by comparison of cross peaks in a NOESY spectrum with those in a TOCSY spectrum acquired under similar experimental conditions (Wuthrich, 1986). 2D-NOESY experiments were performed with 200, 300, 400 and 500 msec mixing times. 2D-TOCSY spectra were recorded using MLEV-17 (Bax & Davis, 1985) for isotropic mixing for 70 msec at a B1 field strength of 8 KHz. Water peak suppression was obtained by low-power irradiation of the H_2O peak during relaxation delay. The TFE peak was considered the reference peak for chemical shift assignment. All experiments were zero-filled to 4K data points in the t1 dimension and when necessary, spectral resolution was enhanced by Lorenzian-Gaussian apodization.

Molecular Modeling

Peptides were built using the Biopolymer module of Sybyl 6.7. Electrostatics were calculated by the Kollman method (Singh & Kollman, 1984) and a distance-dependent dielectric constant was used ($\varepsilon = 4 \times r$) rather than explicit solvation. The peptide geometry was assigned to be α-helical for the M2GlyR segment, based on results from circular dichroism measurements in 50% TFE, which indicated predominantly α-helical secondary structures for the peptides at temperatures up to 70°C (Tomich et al., 1998). The method described by Devi et al. (Devi, Sitaram & Nagaraj, 1998)

was used to obtain structures for molecular dynamics simulations. Briefly, the initial α-helical structures were subjected to 100 iterations of steepest descent minimizations to eliminate bad contacts, followed by 5 cycles of optimizations using the conjugate gradient method until convergence was reached (0.001 kcal/mol/Å). Molecular dynamics simulations of the energy-minimized structures were done for 10 psec at 300 K.

Results

Channel-forming Properties

Results from tightly paired experiments comparing the concentration-dependent effects of CK_4-M2GlyR and NK_4-M2GlyR on I_{SC} have not been previously reported, although results from similar studies have been reported individually (Broughman et al., 2001; Wallace et al., 2000). Experiments were conducted to rule out the possibility that reported differences in concentration dependence resulted from the environment in which the experiments were completed. Monolayers of MDCK cells were mounted in modified Ussing chambers and exposed to 100 μM 1-ethyl-2-benzimidazolinone (1-EBIO) to activate a basolateral K^+ conductance and thus provide additional electrochemical driving force for anion secretion (Devor et al., 1996). This was followed by treatment of the apical surface of MDCK monolayers with increasing concentrations of either CK_4-M2GlyR or NK_4-M2GlyR, during which time I_{SC} was recorded continuously. Consistent with previous reports, 1-EBIO had no effect on basal I_{SC} (Wallace et al., 2000). The concentration-response relationships for CK_4-M2GlyR and NK_4-M2GlyR in the paired experiments are summarized in Figure 1. The results of the paired experiments are similar to the previous reports in that little effect of either CK_4-M2GlyR or NK_4-M2GlyR is observed at concentrations of less than 100 μM. At every concentration tested, the effect of NK_4-M2GlyR on I_{SC} was greater than that of CK_4-M2GlyR.The data were fitted by a modified Hill equation, $I = I_{max} \times (([P]^n) / ([P]^n \times [P_{50}]^n))$ to determine the maximal response (I_{max}), the peptide concentration producing 50% of the maximal response (P_{50}) and the Hill coefficient (n). The resulting parameters for NK_4-M2GlyR (I_{max} = 25.2 ± 10.4 μA, P = 319 ± 192 μM, n = 1.52 ± 0.55) are similar to those reported previously (Broughman et al., 2001, I_{max} = 24.3 ± 0.5 μA, P_{50} = 208 ± 6 μM, and n = 2.6 ± 0.1). The concentration dependence of CK_4-M2GlyR is right-shifted compared to that of NK_4-M2GlyR, with the response at the greatest concentration tested (500 μM) showing no indication of saturation. The experimental data for CK_4-M2GlyR, when fitted by the modified Hill equation, resulted in a substantially greater value for I_{max} (102.5 μA cm^{-2}) than that observed for a variety of agonists and pore-forming peptides (25–30 μA cm^2). Although

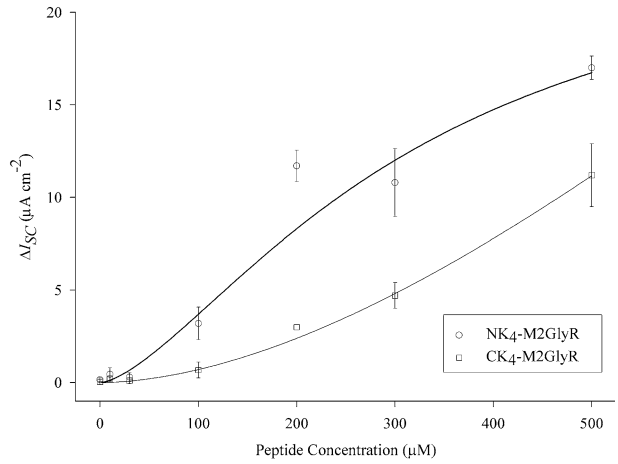

Fig. 1. The dependence of I_{SC} of MDCK monolayers on NK_4-M2GlyR and CK_4-M2GlyR concentration in the presence of 1-EBIO. Values are mean ± SEM for 4 paired experiments. Solid line represents the best fit of a modified Hill equation (*see* Methods) to each of the data sets. The parameters obtained were I_{max} = 25.2 ± 10.4 μA cm^{-2}, P_{50} = 319 ± 192 μM, n = 1.52 ± 0.55 for NK_4-M2GlyR and P_{50} = 553 μM, n = 2.30 ± 1.63 for CK_4-M2GlyR with the I_{max} held constant at 25.2 μA.

this predicted value might be correct, the peptide-induced conductance is, in all likelihood, not rate-limiting for anion-conductance secretion by the epithelial monolayer. Therefore, I_{max} was constrained to the value obtained from the fit to the Hill equation for NK_4-M2GlyR. Using this constraint, the concentration of CK_4-M2GlyR predicted to produce 50% of the maximum response (P_{50}) is 553 μM and the Hill coefficient (n) is 2.30 ± 1.63. These results demonstrate clear differences in the channel-forming activity of NK_4-M2GlyR and CK_4-M2GlyR, based on their ability to increase anion secretion across an epithelial monolayer. These differences could involve a number of properties of the peptides in aqueous or lipid phases including peptide-peptide associations in solution, lipid partitioning, and channel assembly. How the location of the lysine tail alters the structural characteristics of the NK_4-M2GlyR and CK_4-M2GlyR peptides was explored to assess the potential effects of any structural differences on these properties.

Cross-linking and High-Molecular Weight Peptide-Peptide Association

Previously, it was shown that aqueous solubility of NK_4- and CK_4-M2GlyR peptides was greatly enhanced compared to the native M2GlyR sequence. However, TOCSY-NMR studies suggested that there were differences in the behavior of CK_4-M2GlyR and NK_4-M2GlyR in aqueous solution with a higher proportion of CK_4-M2GlyR existing as monomer rather than as soluble associations as compared to NK_4-M2GlyR (Tomich et al., 1998). To explore dif-

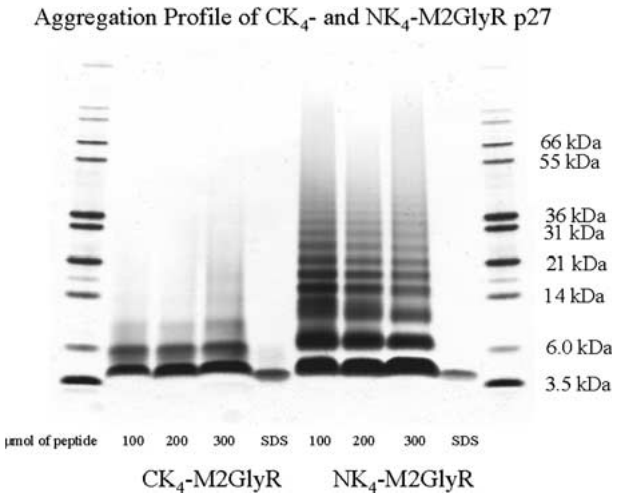

Fig. 2. Silver-stained tricine polyacrylamide gel of NK_4-M2GlyR and CK_4-M2GlyR. Lanes *1* & *10*, molecular weight marker; lanes *2–4*, NK_4-M2GlyR treated with a 40-fold excess of cross-linking reagent (lane *2*, 100 μM; lane *3*, 200 μM; lane *4*, 300 μM); lane *5*, untreated NK_4-M2GlyR boiled in SDS-containing sample buffer; lanes *6–8*, CK_4-M2GlyR treated with a 40-fold excess of cross-linking reagent (lane *6*, 100 μM; lane *7*, 200 μM; lane *8*, 300 μM); lane *9*, untreated CK_4-M2GlyR, boiled in SDS-containing sample buffer.

ferences between the high-molecular weight associations of CK_4-M2GlyR and NK_4-M2GlyR further, solutions of the peptides were reacted with the amino-reactive homo-bifunctional cross-linking reagent, Bis[Sulfosuccinimidyl]suberate (BS^3). This water-soluble reagent forms cross-links between two amino groups through reaction with the sulfo-*N*-hydroxy-succinimidyl ester moieties, resulting in an 11.4-Å link between the reacted residues. The formation of high-molecular weight associations of CK_4-M2GlyR and NK_4-M2GlyR that occur in aqueous solution was determined from SDS-PAGE analysis of the complexes that result from intermolecular cross-linking reactions between the peptides in solution. Figure 2 shows SDS-PAGE analysis of the products of cross-linking reactions for CK_4-M2GlyR and NK_4-M2GlyR. In the absence of the BS^3 cross-linking reagent, CK_4-M2GlyR and NK_4-M2GlyR (Fig. 2, lanes *5* and *9*, respectively) appear as a single band, indicating that any associations of the peptides that exist in aqueous solution are dissociated by boiling in SDS-containing sample buffer. In contrast, the native M2GlyR forms associations that are not dissociated by heating in SDS-containing sample buffer (*data not shown*). Data presented in lanes 2–4 (CK_4-M2GlyR) and lanes 6–8 (NK_4-M2GlyR) indicate that increasing the concentration of dissolved peptide does influence the formation of peptide-peptide associations. Clear differences in the degree of association and/or cross-linking propensities of NK_4-M2GlyR and CK_4-M2GlyR are observed. The NK_4-M2GlyR peptide forms larger cross-linked associations than CK_4-M2GlyR, with masses greater than 30 kDa in water. In contrast, CK_4-M2GlyR cross-linking products correspond to the masses expected for dimer and trimers, with much of the unreacted monomer still present. The observed differences in association are consistent with the previously reported higher solubility of CK_4-M2GlyR, which may be due to a higher percentage of lower-molecular weight complexes (Tomich et al., 1998).

The SDS-PAGE analysis also reveals differences in the electrophoretic mobility of the monomeric forms of NK_4-M2GlyR and CK_4-M2GlyR, which have identical masses (Fig. 2). The monomers for NK_4-M2GlyR and CK_4-M2GlyR run with apparent molecular weights of 4900 and 4650, respectively, values that are greater than that obtained by mass spectrometry (2817 Da.). The differences in electrophoretic mobility suggest that the peptides have non-equivalent Stoke's radii, perhaps due to detergent micelle-induced helical structures formed by the peptides (*data not shown*).

Nuclear Magnetic Resonance

A series of one- and two-dimensional NMR experiments were performed on NK_4- and CK_4-M2GlyR. TOCSY NMR spectra were recorded for NK_4- and CK_4-M2GlyR. Data presented in Fig. 3 show the fingerprint region (NH to Cα and side chain proton connectivity) for 500 MHz ^{1}H 2D-experiments for both peptides recorded in water containing 30% deuterated TFE at 30°C (assignments are shown for the lysine residues). The extent of chemical-shift dispersion of the backbone proton resonances, particularly of the lysine residue amide protons (in spite of the oligomeric nature of the lysines in these sequences), suggest that such a spread of chemical shift can only be induced by secondary structure. However, in comparing the chemical shifts for the lysine residues in the two TOCSY spectra, it is apparent that the environments for these basic amino acids in the two peptides are distinct. For the NH_2-terminal lysine-adducted peptide the dispersion range of the TOCSY chemical shifts for 3 of the 4 lysines was 8.55 to 8.1 ppm. The fourth lysine could not be assigned. In contrast, the COOH-terminal-adducted peptide had a dispersion range of chemical shifts that spanned 8.15–7.72 ppm. All four of the CK_4-M2GlyR lysine resonances were assigned. Greater dispersion in the chemical shift pattern observed with NK_4-M2GlyR indicates that these residues are more mobile than lysine residues adducted to the COOH-terminus.

NOESY experiments were also performed on CK_4-M2GlyR and NK_4-M2GlyR (Fig. 4). The presence of NH-NH cross peaks in the NOESY spectrum collected with 200 msec mixing time for CK_4-M2GlyR indicate that at least two of the COOH-terminal lysines are involved in the turn for-

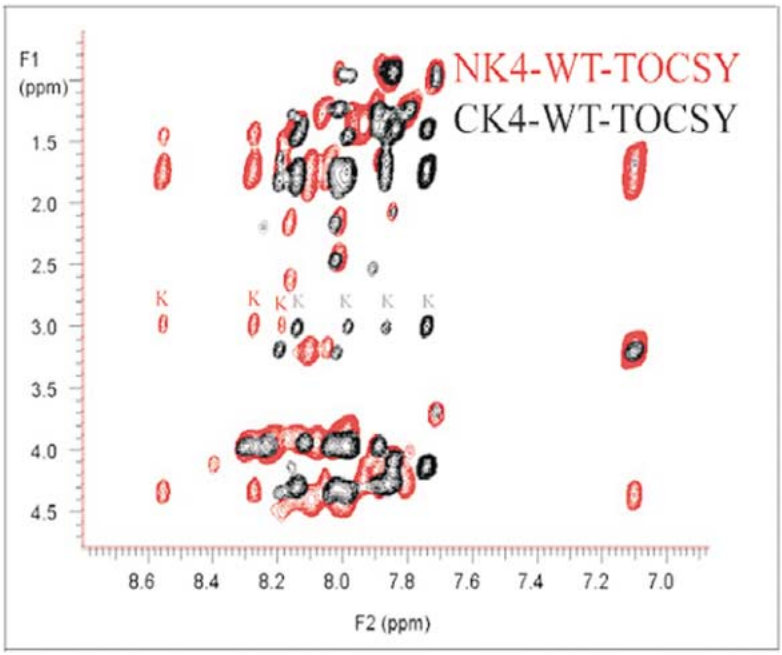

Fig. 3. Fingerprint region (NH to Cα and side-chain proton connectivity) of the 500-MHz TOCSY NMR spectra of NK_4-M2GlyR and CK_4-M2GlyR, recorded under identical conditions in 30% deuterated TFE at 30°C.

mation. No such connectivities were observed for the lysine residues for NK_4-M2GlyR. Two of the lysine residues of CK_4-M2GlyR interact with distant threonine residues. Residues showing common cross peaks in the transmembrane helical segment are indicated. The NH-NH contour plots clearly demonstrate the distinctness of the CK_4-M2GlyR and NK_4-M2GlyR structures.

Molecular Modeling and Dynamics

To gain further insights into the structural differences between CK_4-M2GlyR and NK_4-M2GlyR, these peptides were modeled using a combination of energy-based minimizations and molecular-dynamics simulations. For the starting structures, the residues of the M2GlyR sequence were in an α-helical conformation, while the lysine residues were random coil. After minimizing, the peptides were put through 10-psec molecular dynamics simulations. The ten lowest energy structures were then minimized to obtain the conformers of CK_4-M2GlyR and NK_4-M2GlyR shown in Fig. 5, upper and lower panels, respectively. The lysine residues of CK_4-M2GlyR form a C-cap by extensive interactions with the helix backbone, which remain fairly static throughout the molecular dynamics simulation period. There was very little motion of the helix backbone of CK_4-M2GlyR during the simulation period. In contrast, the lysine residues of NK_4-M2GlyR remained mostly extended away from the helix until several psec into the simulation, interacting minimally with the M2GlyR backbone. The lysine tail of NK_4-M2GlyR eventually folded back to form some interactions with the helix backbone, but to a much lesser extent than CK_4-M2GlyR.

Hydrogen bonds are predicted to be formed by all four of the CK_4-M2GlyR lysine residues, but only by two of the NK_4-M2GlyR lysine residues (Fig. 6). The side chain ε-amino of lys-24 of CK_4-M2GlyR forms a capping structure that stabilizes the helix by forming H-bonds with the backbone carbonyl groups of ser-21, arg-22 and ala-23, fulfilling H-bonding interactions that are absent in the COOH terminal residues of an α-helix. The ε-amino group of lys-25 of CK_4-M2GlyR forms H-bonds with the backbone carbonyl groups of thr-16 and lys-27 and the hydroxyl side chain of thr-16. The ε-amino groups of lys-26 and lys-27 of CK_4-M2GlyR form hydrogen bonds to the backbone carbonyl of lys-25 and the side chain carbonyl of gln-17, respectively. The side chain ε-amino groups of lys-1 and lys-4 of NK_4-M2GlyR do not form H-bonds, as the lysyl residues' side chains extend away from the helix backbone. The ε-amino group of lys-2 forms an H-bond with its own backbone carbonyl. The ε-amino group of lys-3 of NK_4-M2GlyR forms H-bonds with the backbone carbonyl groups of lys-2, lys-3, pro-5 and ala-6. Based on the H-bonding pattern of the backbone amide and carbonyls, NK_4-M2GlyR forms a 3^{10} helix from ala-6 to gly-9 and a normal α-helix from leu-10 to ala-27. CK_4-M2GlyR is in an α-helical conformation from pro-1 to ala-23 with the exception of a kink created near gly-20 that results in a disruption of the amide to carbonyl H-bonding interactions of thr-15 and thr-16.

Large differences are predicted for the dipoles of NK_4-M2GlyR and CK_4-M2GlyR (Fig. 7, left and right panels, respectively). Note the similarities between the dipoles of the unmodified M2GlyR sequence and NK_4-M2GlyR. The dipole of CK_4-M2GlyR is shifted by nearly 90 degrees and is about one third of

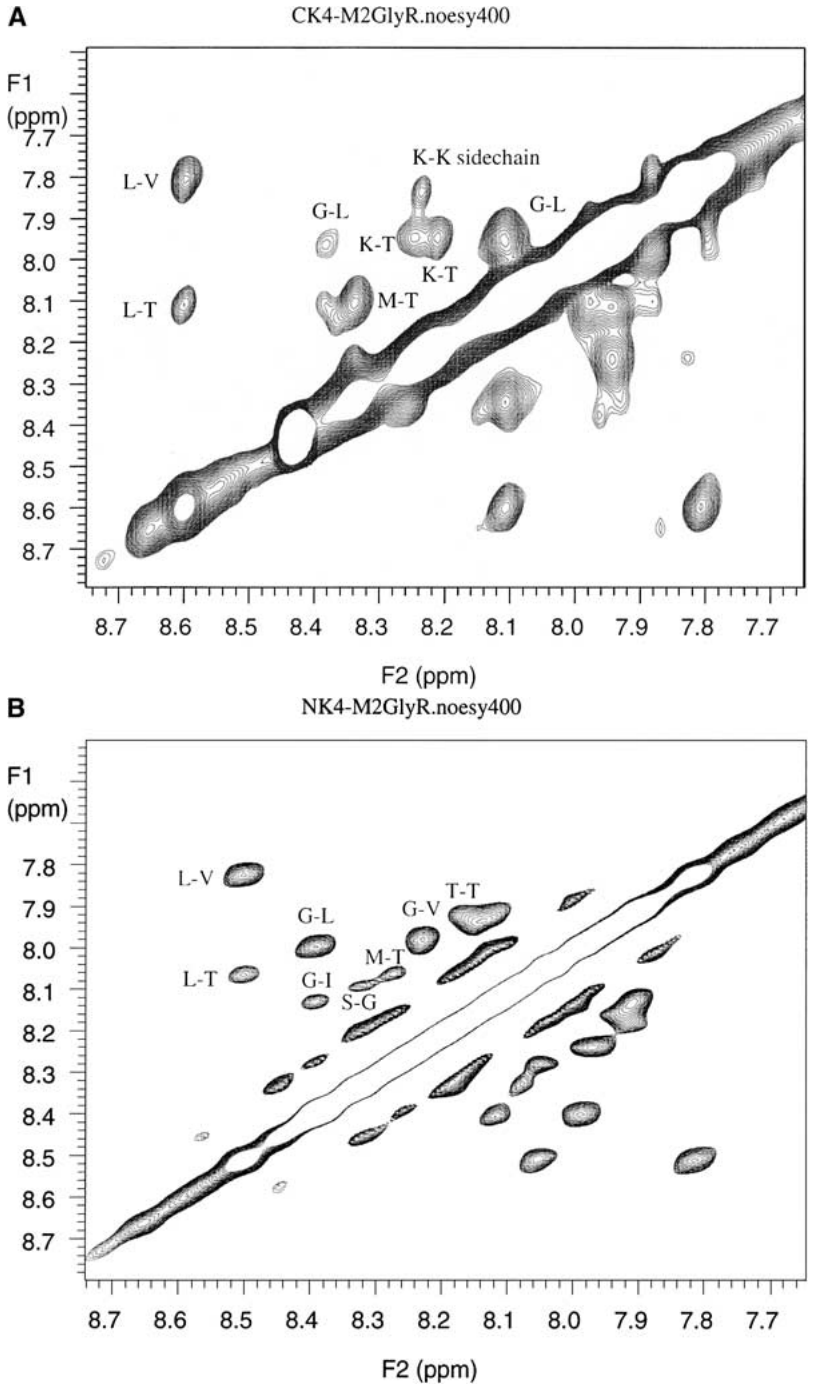

Fig. 4. Fingerprint region of the 500-MHz ^{1}H 2D NOESY NMR spectra of (*A*) CK_4-M2GlyR and (*B*) NK_4-M2GlyR with 200 msec mixing time, recorded under the same conditions as in Figure 3.

the magnitude of the dipole of the parent compound. This perturbation of the dipole could play a role in the differences observed in peptide-peptide association and channel activity of the CK_4-M2GlyR peptide.

Discussion

Previous studies of lysine-modified derivatives of the M2GlyR pore-forming region have demonstrated numerous differences in aqueous solubility, peptide-peptide association, and channel-forming activity. These differences in the biophysical properties of NK_4-M2GlyR and CK_4-M2GlyR must result from differences in the structure of the peptides near the lysine tail and/or interactions of the lysine residues with the helical M2GlyR segment of the peptide. The present study shows differences in the concentration-dependence of peptide-induced increases in I_{SC} and cross-linking of peptide-peptide associations, and explores the structural differences of the peptides by NMR and molecular modeling that may account for

Fig. 5. Stick representations of ten lowest-energy conformers of CK_4-M2GlyR (*top*) and NK_4-M2GlyR (*bottom*) from molecular dynamics simulations at 300 K for 10 psec. The lysine residues on the CK_4-M2GlyR molecule interact with the side chain of threonine 15, as seen in the NOESY NMR spectra. The lysine residues of NK_4-M2GlyR extend away from the molecule and have considerably more freedom than the lysines of CK_4-M2GlyR. Both structures are modeled to the same scale.

the distinct biophysical and channel-forming properties of NK_4-M2GlyR and CK_4-M2GlyR.

An important factor influencing the interpretation of these results is the nature of the environment in which the experiments were conducted. The peptide is delivered from a high-dielectric aqueous environment to a membrane environment that has a low-dielectric core flanked by regions of increasing dielectric and aqueous solution. In this environment the peptides are able to form functional channels. The previous CD and current NMR studies were carried out in the presence of TFE, which induces the peptide to form a helical structure, but certainly cannot mimic the complexities of a biological membrane. Another confounding factor in the interpretation of these results is the presence of soluble complexes in solution. In a previous study, (Tomich et al., 1998) NK_4-M2GlyR consistently showed an increased viscosity compared to CK_4-M2GlyR. These data suggest that the energy required to break the capping structure to form a species of the peptide that is capable of insertion into the membrane is the determining factor. An alternative explanation of these results is that the equilibrium between peptide in aqueous solution and peptide associated with the membrane is shifted towards the aqueous state for CK_4-M2GlyR.

The current study provides further support for differences in the ability of CK_4-M2GlyR and NK_4-M2GlyR to stimulate increases in I_{SC} across MDCK monolayers (Broughman et al., 2001; Wallace et al., 2000). Results from the tightly paired experiments show that both orientations of the peptide have a concentration-dependent ability to induce an I_{SC} across epithelial cell monolayers. Assuming that the energy barrier for the translocation of the four lysine residues across the hydrophobic membrane is prohibitive (Vogt et al., 2000), either orientation (NH_2 or COOH terminal towards extracellular surface) can insert into the membrane and assemble into an anion-conducting pore. However, based on the observation that the concentration required to produce 50% of the maximum increase in I_{SC} for NK_4-M2GlyR is one-third less than that required for CK_4-M2GlyR (P_{50} = 319 μM *vs.* 553 μM, respectively), the efficiency of the insertion or the assembly of these two peptides

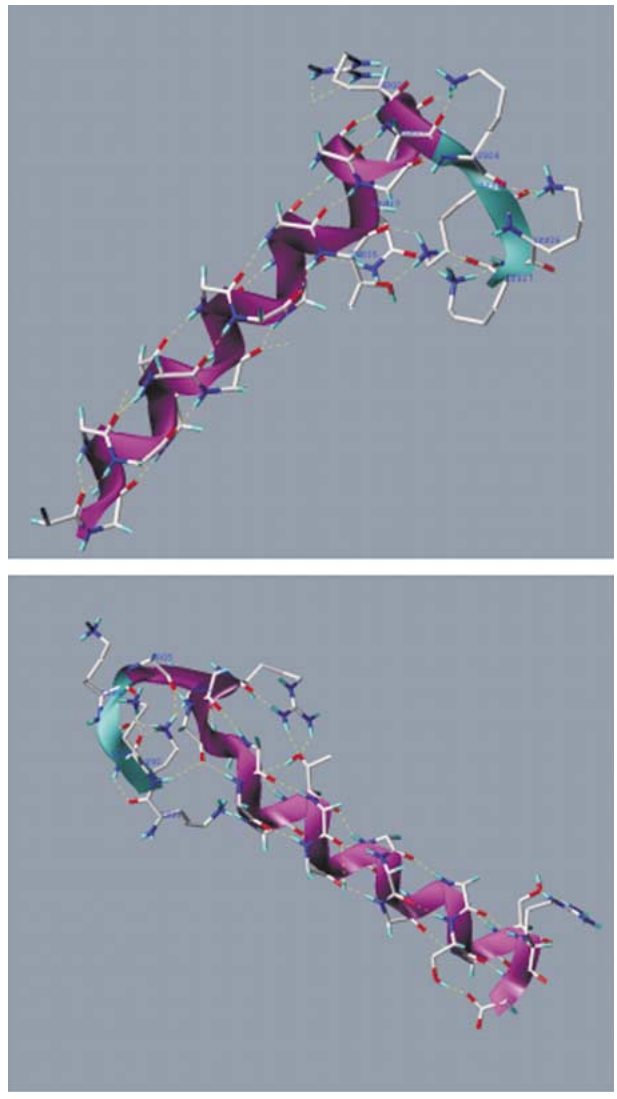

Fig. 6. The hydrogen bonds predicted for CK_4-M2GlyR (*top*) and NK4-M2GlyR (*bottom*). The average conformation from an RMSD alignment of the ten lowest-energy conformers is shown as a ribbon structure with only side chain residues involved in H-bonding shown for clarity. The dotted yellow lines designate the predicted hydrogen bonds.

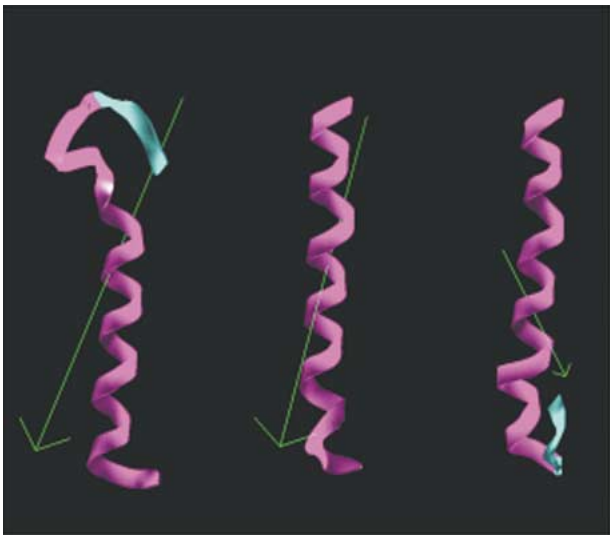

Fig. 7. The dipole moments of NK_4-NKGlyR (*left*), M2GlyR (*center*) and CK_4-M2GlyR (*right*) are shown as ribbon structures (magenta is helix and cyan is random coil) with the dipoles represented by green arrows. For this representation, the dipoles of NK_4-M2GlyR and M2GlyR were scaled down by a factor of 20, while the dipole for CK_4-M2GlyR was scaled up by a factor of 3.

into channel-forming structures is not equivalent. Furthermore, the concentration-dependent effects of the peptides on I_{SC} show a smaller Hill coefficient for NK_4-M2GlyR than CK_4-M2GlyR (n = 1.5 *vs.* 2.3, respectively). This suggests that one or more of the steps required for channel assembly (e.g., insertion, oligomerization) is more cooperative in the case of CK_4-M2GlyR. Alternatively, as NK_4-M2GlyR is less soluble than CK_4-M2GlyR in aqueous solution, the hydrophobic driving force for the insertion of NK_4-M2GlyR into the membrane is greater. In either case, structural differences between the lysine-modified peptides result in altered channel-forming activity. How the location of the lysine residues on the M2GlyR pore sequence could potentially affect these processes was explored further by investigating the oligomeric state of the peptides in aqueous solution by chemical cross-linking and SDS-PAGE analysis.

Initially, we hypothesized that the low-molecular weight forms of the peptides (monomer and dimer) in aqueous solution were the active forms of the peptide, capable of partitioning into lipid bilayers and channel assembly. Thus, the greater the proportion of peptide monomers in solution, the greater the channel-forming activity predicted. We also surmised that the lysine residues at the COOH-terminus somehow either interfered with channel assembly or possibly increased peptide-peptide associations, resulting in less efficient membrane partitioning. The cross-linking experiments with BS^3 indicated that, in fact, CK_4-M2GlyR had fewer higher-order complexes and an increased population of monomer compared to NK_4-M2GlyR, which existed as primarily dimers, trimers and higher-order associations. This result suggests that there may be a nucleation site for self-association of the peptide, located near the COOH-terminus of the M2GlyR sequence that is masked by the lysine tail at the COOH-terminus, which prevents formation of higher order assemblies by CK_4-M2GlyR. In the case of NK_4-M2GlyR, the nucleation site remains exposed, resulting in the formation of oligomeric assemblies of NK_4-M2GlyR that can be cross-linked by BS^3. There are alternative explanations for the differences observed in the cross-linking of CK_4-M2GlyR and NK_4-M2GlyR. Hydrogen bonding interactions by the ε-amino groups of lysine residues at the COOH-terminus may result in their unavailability to the cross-linking agent. The CK_4-M2GlyR may, in fact, form higher-molecular weight associations, but with the lysine residues buried and inaccessible to the BS^3 reagent. Any of these explanations implies that the structure of the lysine tail at the COOH- *vs.* the NH_2-terminus of the M2GlyR sequence imparts very different properties to the peptide. We sought insight into the structural basis of these differences using NMR analysis and molecular modeling of CK_4-M2GlyR and NK_4-M2GlyR structures.

NMR analysis revealed differences in both the flexibility of the lysine residues and secondary structure of CK_4-M2GlyR and NK_4-M2GlyR. The TOCSY spectrum of NK_4-M2GlyR has a more disperse chemical shift pattern than that of CK_4-M2GlyR, suggesting that lysine residues of NK_4-M2GlyR are more mobile than lysine residues adducted to the COOH-terminus. The NOESY spectrum of CK_4-M2GlyR indicates that at least two of the COOH-terminal lysines are involved in the turn formation, interacting with threonine residues that are near the middle of the peptide sequence. Similar connectivities are not observed for the lysine residues of NK_4-M2GlyR. These results show that the environments of the lysine residues in the two peptides are distinct. On the basis of these differences, we created molecular models and performed molecular dynamics simulations for both the NH_2- and COOH-lysyl-adducted structures. Consistent with the NMR studies, molecular dynamics simulations suggest that the lysine residues of CK_4-M2GlyR forms stable hydrogen bonds, resulting in a more compact structure than that of NK_4-M2GlyR. In addition, NK_4-M2GlyR has less disruption to the amphipathic helical portion (the M2GlyR sequence) than has CK_4-M2GlyR. These structural differences offer potential explanations for the distinct biophysical characteristics of the two peptides.

The extended conformation of NK_4-M2GlyR may be more stable in the bilayer than the compact, CK_4-M2GlyR peptide. The model structures of CK_4-M2GlyR and NK_4-M2GlyR shown in Fig. 7 suggest the transbilayer orientation of CK_4-M2GlyR peptide may be less stable due to the interactions of the lysine

residues with the backbone carbonyl oxygens. This may explain the observation that NK_4-M2GlyR forms more stable channels in planar lipid bilayers compared to CK_4-M2GlyR and the increased channel-forming activity of NK_4-M2GlyR in epithelial cells (Fig. 1) (Broughman et al., 2001; Mitchell et al., 2000). By not being constrained as in CK_4-M2GlyR, the lysines at the NH_2-terminal may actually stabilize the peptide in the bilayer (de Planque et al., 1999), resulting in enhanced channel-forming activity at lower peptide concentrations.

The differences in the self-association of NK_4-M2GlyR and CK_4-M2GlyR may be explained by differences in the lysine interactions with the helical M2GlyR region. The flexible lysine residues of NK_4-M2GlyR are readily available to amino-reactive cross-linking reagents, whereas the lysine residues of CK_4-M2GlyR form a cap-like structure with strong hydrogen bonds to helix residues, and may thus be less reactive with cross-linking reagents. Another explanation of these results is that a nucleation site for association may be masked by the cap structure at the COOH-terminus. This supports the latter explanation if one assumes that the molecular interaction site in aqueous solution (resulting in self-association) and lipid environment (resulting in channel assembly) is the same.

In summary, poly-lysine tails interact more extensively with an α-helical sequence at the COOH-terminus than at the NH_2-terminus. Modeling and NMR data suggest that lysine residues at the COOH-terminus may form a hydrogen-bonded cap structure that turns back toward the helix, while lysine residues at the NH_2-terminus are flexible and do not interact extensively with the helix residues. For the M2GlyR α-helical pore-forming sequence, modification with lysine residues at the COOH- or NH_2-terminus results in peptides with distinct biophysical characteristics (self-association, solubility) and channel-forming properties that can be explained in terms of structural differences between the CK_4-M2GlyR and NK_4-M2GlyR that are shown in the present study by NMR analysis and molecular modeling. Based on this study and studies on amino-acid substitutions and deletions of these peptide sequences (Broughman et al., 2002), it is clear that the NH_2-terminal-modified adducts are better candidates for further development as agents for channel replacement therapy.

We gratefully acknowledge Dr. Lisa Freeman for her thoughtful discussions and Gary Radke, Ryan Carlin and Yuxi Gong for their indispensable technical help during the progress of this study and preparation of this manuscript. The work was supported by NIH grants NIGMS-RO143617 and NMR structural supplement (JMT), F32GM19332 (KEM), and the Kansas Agricultural Experimental Station (KAES manuscript no. 02-126-J).

References

Aurora, R., Rose, G.D. 1998. Helix capping. *Protein Sci.* **7:**21–38

Bax, A., Davis, D. 1985. MLEV-17 based two-dimensional homonuclear magnetization transfer spectroscopy. *J. Magn. Reson.* **65:**355–360

Bohm, G., Muhr, R., Jaenicke, R. 1992. Quantitative analysis of protein far UV circular dichroism spectra by neural networks. *Protein Eng.* **5:**191–195

Broughman, J.R., Mitchell, K.E., Sedlacek, R.L., Iwamoto, T., Tomich, J.M., Schultz, B.D. 2001. NH_2-terminal modification of a channel-forming peptide increases capacity for epithelial anion secretion. *Am. J. Physiol.* **280:**C451–C458

Broughman, J.R., Shank, L.P., Takeguchi, W., Schultz, B.D., Iwamoto, T., Mitchell, K.E., Tomich, J.M. 2002. Distinct structural elements that direct solution aggregation and membrane assembly in the channel-forming peptide M2GlyR. *Biochemistry* **41:**7350–7358

de Planque, M.R., Kruijtzer, J.A., Liskamp, R.M., Marsh, D., Greathouse, D.V., Koeppe 2nd, R.E., de Kruijff, B., Killian, J.A. 1999. Different membrane anchoring positions of tryptophan and lysine in synthetic transmembrane alpha-helical peptides. *J. Biol. Chem.* **274:**20839–20846

Devi, A.S., Sitaram, N., Nagaraj, R. 1998. Structural features of helical aggregates of antibacterial peptides via simulated annealing and molecular modeling. *J. Biomol. Struct. Dyn.* **15:**653–661

Devor, D.C., Singh, A.K., Frizzell, R.A., Bridges, RJ. 1996. Modulation of Cl-secretion by benzimidazolones. I. Direct activation of a Ca(2+)-dependent K^+ channel. *Am. J. Physiol.* **271:**L775–L784

Esposito, G., Dhanapal, B., Dumy, P., Varma, V., Mutter, M., Bodenhausen, G. 1997. Lysine as helix C-capping residue in a synthetic peptide. *Biopolymers* **41:**27–35

Gao, L., Broughman, J.R., Iwamoto, T., Tomich, J.M., Venglarik, C.J., Forman, H.J. 2001. Synthetic chloride channel restores glutathione secretion in cystic fibrosis airway epithelia. *Am. J. Physiol.* **281:**L24–L30

Mitchell, K.E., Iwamoto, T., Tomich, J., Freeman, L.C. 2000. A synthetic peptide based on a glycine-gated chloride channel induces a novel chloride conductance in isolated epithelial cells. *Biochim. Biophys. Acta* **1466:**47–60

Presta, L.G., Rose, G.D. 1988. Helix signals in proteins. *Science* **240:**1632–1641

Reddy, G.L., Iwamoto, T., Tomich, J.M., Montal, M. 1993. Synthetic peptides and four-helix bundle proteins as model systems for the pore-forming structure of channel proteins. II. Transmembrane segment M2 of the brain glycine receptor is a plausible candidate for the pore-lining structure. *J. Biol. Chem.* **268:**14608–14615

Richardson, J.S., Richardson, D.C. 1988. Amino acid preference for specific locations at the ends of alpha helices. *Science* **240:**1648–1652

Schagger, H., von Jagow, G. 1987. Tricine-sodium dodecyl sulfate-polyacrylamide gel electrophoresis for the separation of proteins in the range from 1 to 100 kDa. *Anal. Biochem.* **166:**368–379

Singh, U., Kollman, P. 1984. An approach to computing electrostatic charges for molecules. *J. Comput. Chem.* **5:**129–145

Tomich, J.M., Wallace, D., Henderson, K., Mitchell, K.E., Radke, G., Brandt, R., Ambler, C.A., Scott, A.J., Grantham, J., Sullivan, L., Iwamoto, T. 1998. Aqueous solubilization of transmembrane peptide sequences with retention of membrane insertion and function. *Biophys. J.* **74:**256–267

Vogen, S.M., Prakash, O., Kirnarsky, L., Sanderson, S.D., Sherman, S.A. 1998. NMR analysis of a potent decapeptide agonist of human C5a anaphylatoxin. *J. Pept. Res.* **51:**226–234

Vogt, B., Ducarme, P., Schinzel, S., Brasseur, R., Bechinger, B. 2000. The topology of lysine-containing amphipathic peptides in bilayers by circular dichroism, solid-state NMR, and molecular modeling. *Biophys. J.* **79:**2644–2656

Wallace, D.P., Tomich, J.M., Eppler, J.W., Iwamoto, T., Grantham, J.J., Sullivan, L.P. 2000. A synthetic channel-forming peptide induces Cl(−) secretion: modulation by Ca(2+)-dependent K(+) channels. *Biochim. Biophys. Acta* **1464:**69–82

Wallace, D.P., Tomich, J.M., Iwamoto, T., Henderson, K., Grantham, J.J., Sullivan, L.P. 1997. A synthetic peptide derived from glycine-gated Cl-channel induces transepithelial Cl- and fluid secretion. *Am. J. Physiol.* **272:**C1672–C1679

Wuthrich, K. 1986. NMR of Proteins and Nucleic Acids. John Wiley & Sons, New York

Zhou, W., Flanagan, C., Ballesteros, J.A., Konvicka, K., Davidson, J.S., Weinstein, H., Millar, R.P., Sealfon, S.C. 1994. A reciprocal mutation supports helix 2 and helix 7 proximity in the gonadotropin-releasing hormone receptor. *Mol. Pharmacol.* **45:**165–170